



ELSEVIER

Journal of Volcanology and Geothermal Research 119 (2002) 145–159

Journal of volcanology
and geothermal research

www.elsevier.com/locate/jvolgeores

Effects of regional slope on viscous flows: a preliminary study of lava terrace emplacement at submarine volcanic rift zones

Wenlu Zhu^{a,*}, Deborah K. Smith^a, Laurent G.J. Montési^b

^a Department of Geology and Geophysics, Woods Hole Oceanographic Institution, Woods Hole, MA 02543, USA

^b Department of Earth, Atmospheric and Planetary Sciences, Massachusetts Institute of Technology, Cambridge, MA, USA

Received 10 February 2001; accepted 4 April 2002

Abstract

To understand how large submarine lava terraces form and why they are not commonly observed on land, we developed an isoviscous gravity flow model on an inclined surface to simulate the evolution and emplacement of lava flows under submarine conditions. By solving this preliminary model using a finite difference method, we are able to quantify how lava viscosity, pre-existing topographic slope, effusion rate, and lava volume affect meso-scale lava morphology. Our simulations show that, in general, high lava viscosity, gentle regional slope, and low effusion rate favor the formation of large terraces, but environmental conditions also play an important role. A gravity flow spreads more slowly underwater than subaerially. We also conclude that for low viscosity basaltic lava, the cooling of the lava body is one of the most critical factors that affect its shape. This study shows that the isoviscous model, though oversimplified, provides a quantitative tool to relate lava morphology to eruption characteristics. To gain a better understanding of the controls on submarine lava terrace formation, future models must take into account the temporal and spatial variation of lava viscosity, especially the effects of a brittle outer shell.

© 2002 Elsevier Science B.V. All rights reserved.

Keywords: gravity flow; submarine terraces; volcanic zones; Puna Ridge; Hawaii

1. Introduction

It is important to obtain a good understanding of the parameters that control the shapes of basaltic lava eruptions at submarine rift zones in order to answer many fundamental questions concerning rift zone dynamics. Why do low-relief flows mantle the topography in some places, and

large lava terraces, which are up to several kilometers in diameter and up to several hundreds of meters high, form in other places? Is it mostly the result of differing lava viscosity, ambient pressure, lava volume, how steady the flow is, pre-existing slope, or effusion rate? Is it some combination of these parameters that is important? Answering questions such as these will help us judge how confidently we can infer eruption variables from the resulting submarine volcanic morphology. This issue has generated a lot of discussion recently as attempts have been made to constrain

* Corresponding author.

E-mail address: wzhu@whoi.edu (W. Zhu).

the dynamics of newly emplaced lava flows observed at mid-ocean ridges, such as the fast-spreading East Pacific Rise (e.g. Haymon et al., 1993) and the intermediate-spreading Juan de Fuca Ridge (e.g. Chadwick and Embley, 1998), and their relationship to subsurface crustal processes such as magma supply and dike emplacement (e.g. Perfit and Chadwick, 1998).

Detailed images of the seafloor around the Hawaiian Islands show that flat-topped volcanic cones and domes are commonly constructed on the submarine flanks and rift zones of the Hawaiian volcanoes (e.g. Smith and Cann, 1999; Clague et al., 2000; Smith et al., 2002). We refer to these cones and domes as *terraces* to reflect the fact that they form on slopes and their flat tops are remarkably horizontal (Figs. 1 and 2). While terraces are abundant on the seafloor of the Hawaiian submarine rift zones, they are rare in subaerial basaltic flows (e.g. Clague et al., 2000). Interestingly, these flat-topped volcanoes are also fre-

quently observed at slow-spreading mid-ocean ridges (e.g. Smith and Cann, 1999; Smith et al., 2002) and ultra-slow-spreading ridges (Nancy Grindlay, personal communication), whereas they are not common at fast-spreading ridges (e.g. Perfit and Chadwick, 1998). What does their formation tell us about how these submarine rift zones work?

Small-scale aspects of submarine flow dynamics, such as why pillows form instead of sheet flows, have been investigated (e.g. Moore et al., 1973; Griffiths and Fink, 1992; Gregg and Fink, 1995), but the controls on the forms of larger volcanic edifices that are hundreds of meters to kilometers in diameter are not well understood, and it is this latter scale on which we focus our study. There have been a few theoretical and experimental models developed to understand the construction of lava domes associated with large, explosive subaerial volcanoes (e.g. Huppert et al., 1982). Since submarine terraces are morphologi-

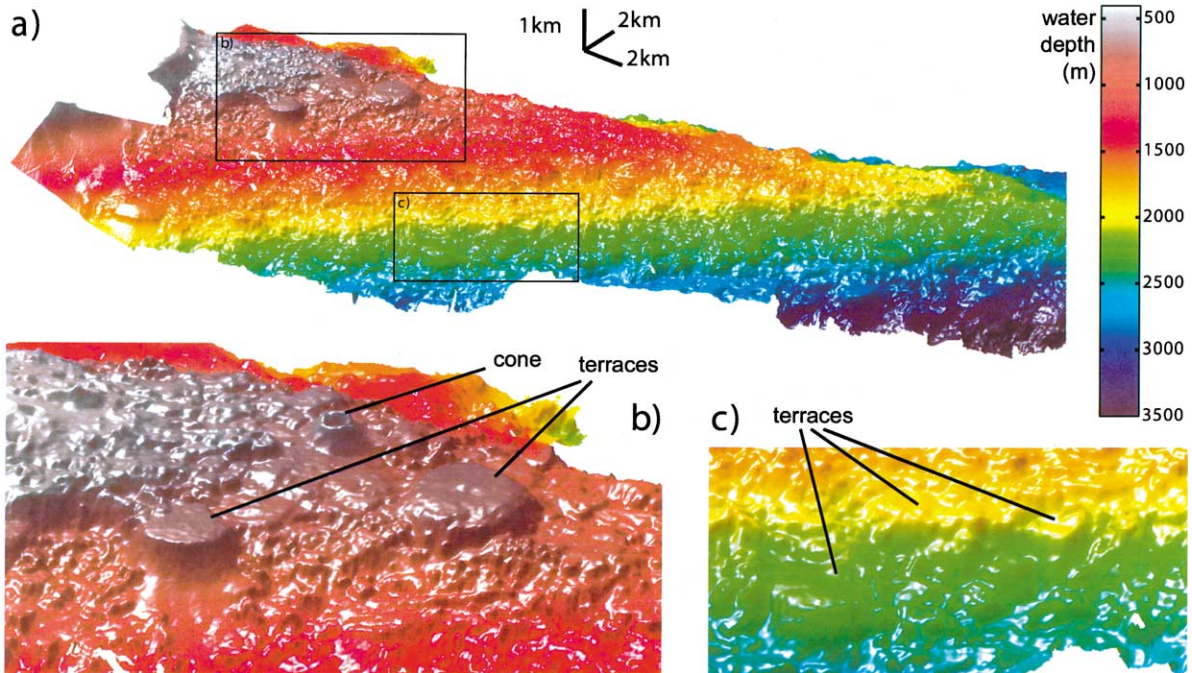


Fig. 1. (a) 3-D view of the Puna Ridge, Hawaii from the North. Vertical exaggeration $2\times$. Reconstructed based on bathymetry data from Monterey Bay Aquarium Research Institute Mapping Team (2000). Close up of (b) the summit area and (c) the flank of the ridge. Note the numerous terraces and the paucity of cones, especially on the flanks and at depth. Some terraces appear more eroded than others (note the rubble pile below the left terrace in panel b).

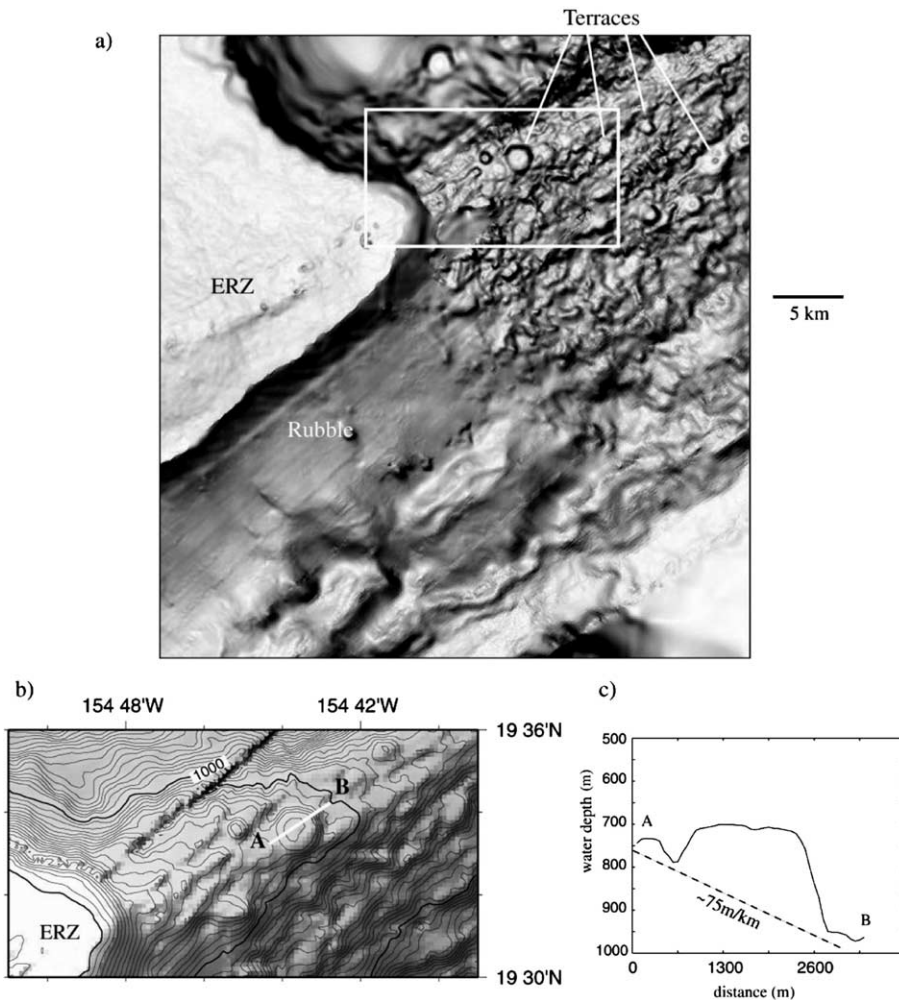


Fig. 2. (a) Slope map of the Puna Ridge from Moore and Chadwick (1995). Dark represents steep slopes, light represents shallow slopes. Note the dramatic change in volcanic morphology between the subaerial ERZ and the submarine Puna Ridge. The top and flanks of the Puna Ridge are covered by lava terraces of all sizes, some of which are marked. The white box shows the location of panel b. (b) Bathymetry map of a section of the upper Puna Ridge contoured at 50-m contour intervals. The dark lineation near the 1000-m label is the seam between two different data sets. The white line across the terrace at the summit of the ridge shows the location of the profile given in panel c. (c) Profile of an on-axis terrace. Note that it has formed on a pre-existing slope (~ 75 m/km, $\sim 4^\circ$). This yields a shape that is asymmetric in cross-section. The relief on the upslope side is much less than on the downslope side.

cally similar to subaerial lava domes, in this study, we start with the existing fluid mechanics models for subaerial domes and expand them to investigate the formation of submarine terraces. In order to constrain the parameters of our models we use data collected at Kilauea Volcano, Hawaii.

2. Submarine lava terraces at the Puna Ridge

In October of 1998, we completed a detailed mapping of the Puna Ridge, Hawaii (Smith et al., 2002). Puna Ridge is the submarine extension of Kilauea Volcano's East Rift Zone (ERZ). It extends ~ 75 km from the shoreline to its distal

end, plunging from sea level to a depth of 5400 m. We surveyed the entire axis of the Puna Ridge and a large section of the south flank using the DSL 120-kHz high-resolution side-scan sonar system and ARGO II photo-imagery system to obtain multi-scale information on lava morphology. Wax cores and dredged rock samples were also collected for geochemical analyses. Below we describe first what other studies have noted about the morphology at the Puna Ridge and then describe what we learned from our high-resolution data set.

2.1. Previous studies at the Puna Ridge

What is intriguing about the volcanic morphology of the Puna Ridge is that while the flow features at the scale of a few meters are very similar

to those observed on the subaerial ERZ, at the meso-scale of a few kilometers they are notably different (e.g. Moore and Chadwick, 1995; Smith and Cann, 1999; Clague et al., 2000). This is despite the fact that the ERZ and the Puna Ridge are constructed in the same way, by lavas erupted along a rift zone.

Lavas erupted at the subaerial ERZ form smooth, low-angle slopes. Gently dipping low-relief lava flows drape the slopes. Large edifices are not commonly observed. If they are constructed, they are eroded by subsequent flows. As an example, the current vent, Pu'u O'o, which at times has reached 200 m in height, has been built and destroyed several times during the last 16 years. The average along- and cross-axis slopes of the Puna Ridge ($\sim 3^\circ$ and 11° respectively) are both steeper and more irregular at a scale of 1–2 km. Flat-

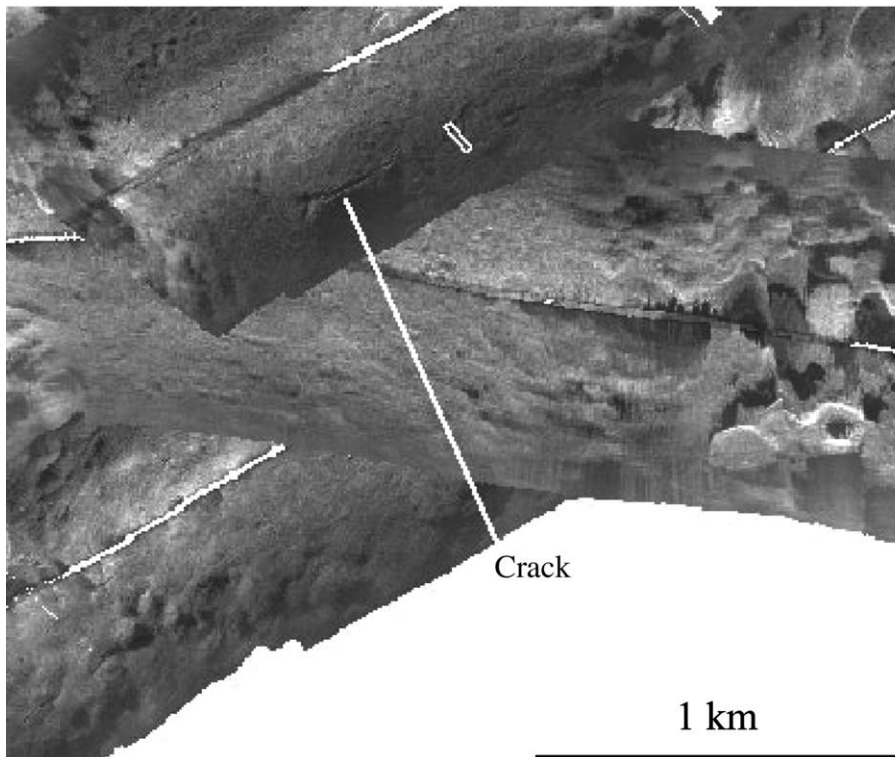


Fig. 3. Mosaic of several DSL 120-kHz side-scan sonar swaths over the top of the large terrace shown in Fig. 2. Each swath is 1 km wide. The region of no data in the center of each swath is directly below the towed vehicle. Although the top of the terrace is covered by a range of lava morphologies (pillows, lobates, sheets), they cannot be distinguished on the side-scan imagery. Inflationary features have formed on the top of the terrace. Note the crack that is marked. We interpret it to be a collapsed tumulus. The white rectangle shows the approximate location of the photo-mosaic shown in Fig. 4.

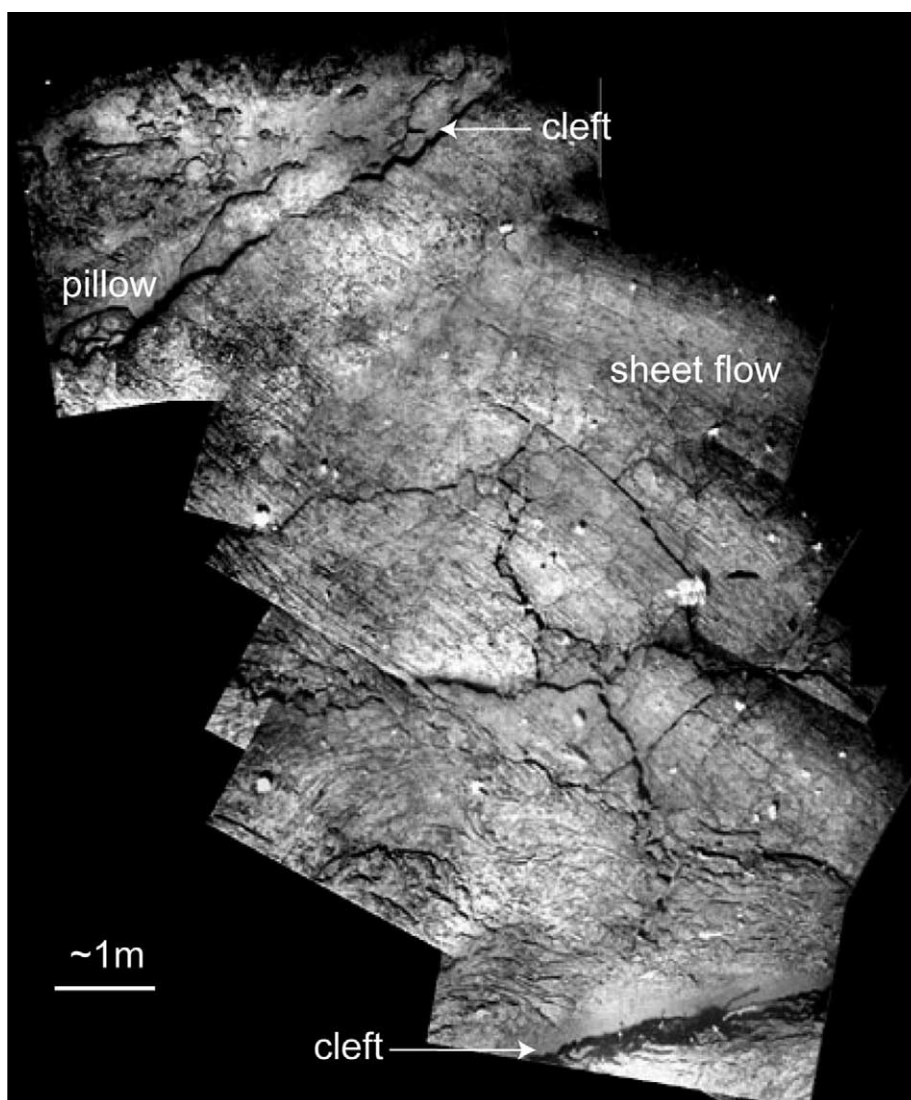


Fig. 4. Mosaic of several ARGON II photographs of the top of a large terrace. High-resolution surveys of the tops of several terraces show that they are coated by a mixture of pillow lavas, lobate flows, and sheet flows. Notice the inflation clefts (tumuli) (Walker, 1991). The cleft at the top of the mosaic has lava squeezing up through it.

topped terraces cover the axis and flanks over its entire length (Fig. 1). The dimensions of these terraces can be up to several kilometers in basal diameter and up to several hundreds of meters high (Fig. 2). One of the interesting features of the terraces is that their top surfaces are usually horizontal (instead of parallel to the overall topographic slope) (Fig. 2c). They are also remarkably

symmetric (near-circular) in plan shape. A sampling of the sizes of terraces that we have identified yields volumes from 0.01 km^3 up to 1 km^3 . Volumes of the most common sized terraces ($\sim 50\text{--}100 \times 10^6 \text{ m}^3$) are similar to those of sustained subaerial eruptions ($\sim 160 \times 10^6 \text{ m}^3$ at Mauna Ulu during 1972–1974; e.g. Tilling et al., 1987). This suggests that all, or at least most, of

the lava that would on the subaerial ERZ produce a broad flow field is focused into a single structure. Why does lava become focused underwater?

2.2. High-resolution side-scan sonar and photo-imagery data

High-resolution surveys of the tops of several terraces show that they are coated by a mixture of pillow lavas, lobate flows, and sheet flows (Figs. 3 and 4). On a larger scale there appear to be two morphological types of flat top: (1) those with one or more summit craters, many of which are eruptive vents as indicated by the lava tubes that lead radially away from them and (2) those with a topographic high or dome near the center. Inflation clefts (or tumuli) are common on the second type and probably formed over lava tubes (Walker, 1991). Our interpretation of the formation of these large terraces follows that of Smith and Cann (1999) and Clague et al. (2000). Terraces are fed from restricted vents (point source) formed from an initial fissure eruption or where a lava tube breaks on the flanks of the ridge. They are monogenetic; that is they are built during a single eruption that might be composed of many episodes. They form during long-lived eruptions with low to moderate effusion rates and grow up-

ward and outward through inflation from within. Eruptions will from time to time coat the top surface of the terrace and its steep flanks. If fluid lava remains within the interior of a terrace, the lava may drain away and form a summit crater. Our model assumptions as described below are based on the above understanding of terrace formation.

3. Isoviscous gravity currents over an inclined surface

Several existing theoretical and experimental models have been constructed to investigate the shapes of dense fluids through time as they are emplaced on rigid surfaces (Fig. 5) (e.g. Huppert, 1982; Huppert et al., 1982; Liu and Mei, 1989; Blake, 1990; Iverson, 1990; Lister, 1992; Berco- vici, 1994; Fink and Griffiths, 1998). These models have been applied to the formation of subaerial lava domes, Venusian ‘pancake’ domes, and mudflows (e.g. Huppert et al., 1982; Pavri et al., 1992; Sakimoto and Zuber, 1995; Liu and Mei, 1989). Lava terraces at the Puna Ridge are emplaced on topographic slopes ranging between 50 and 200 m/km (~3°–11°). Therefore, we use a theoretical model designed to understand how vis-

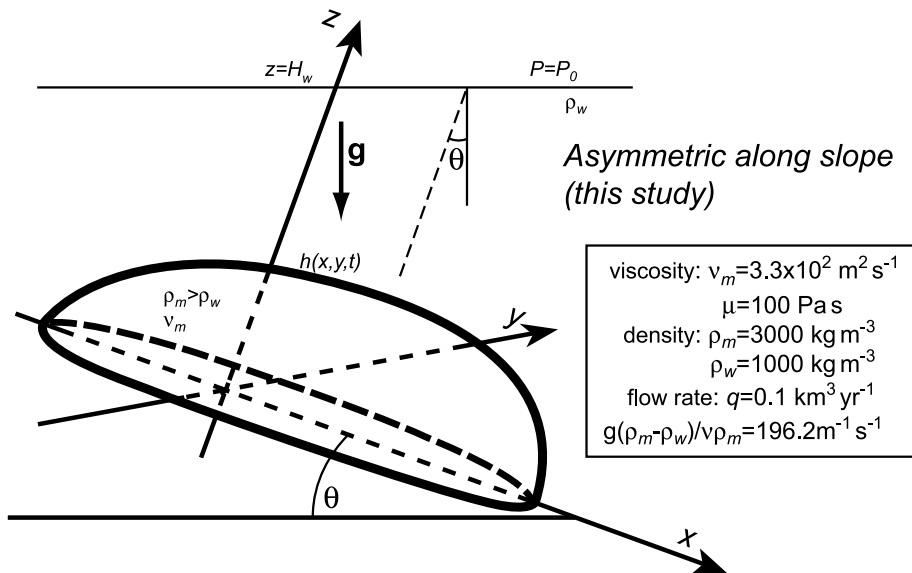


Fig. 5. Schematic diagrams of isoviscous gravity flow spreading on an inclined surface.

cous flows spread on an inclined plane, and adapt it to the submarine environment.

We consider a fluid of constant density (ρ_m) and kinematic viscosity ν that is intruding another fluid with density of ρ_w on a plane inclined at an angle θ to the horizontal. Cartesian coordinates are used, with x along the slope, y across the slope and z perpendicular to the slope surface xy plane (Fig. 5b). The fluid pressure field is:

$$p = [(H_w - z)\cos\theta + x\sin\theta - \frac{1}{\cos\theta}(h - z)]\rho_w g + \frac{1}{\cos\theta}(h - z)\rho_m g \quad (1)$$

In Eq. 1, H_w and h are water depth (constant) and flow thickness, respectively. The implicit assumption used to calculate the pressure field is that the curvature of the surface of the intruding flow is negligible, a valid assumption when the intruding flow is thin (see Liu and Mei, 1989; Lister, 1992) except at the flow edges. From conservation of momentum, the velocity field (with two components, $u(x, z, t)$ in the x direction, and $v(y, z, t)$ in the y direction) can be described as:

$$\begin{aligned} \frac{\partial^2 u}{\partial z^2} &= \frac{g}{\nu} \frac{(\rho_m - \rho_w)}{\rho_m} \left(\frac{1}{\cos\theta} \frac{\partial h}{\partial x} - \sin\theta \right) \\ \frac{\partial^2 v}{\partial z^2} &= \frac{g}{\nu} \frac{(\rho_m - \rho_w)}{\rho_m} \left(\frac{1}{\cos\theta} \frac{\partial h}{\partial y} \right) \end{aligned} \quad (2)$$

While the gravity flow retains its cross-slope symmetry (y direction) over an inclined surface, it becomes asymmetrical along-slope (x direction) because of the last term ($\sin\theta$) on the right hand side of the first half of Eq. 2: the gravity (body force) that will drive the lava flow downhill.

The continuity equation for incompressible flow requires:

$$\frac{\partial h}{\partial t} + \left(\frac{\partial}{\partial x} + \frac{\partial}{\partial y} \right) \int_0^h u dz = 0 \quad (3)$$

We integrate Eq. 2 using a no-slip boundary condition at the bottom (i.e. $u|_{z=0} = 0$) of the spreading flow and a shear free boundary condition on

the top (i.e. $\partial u / \partial z|_{z=h} = 0$). Eq. 3 then becomes the spreading equation:

$$\begin{aligned} \frac{\partial h}{\partial t} &= \frac{1}{3} \frac{g}{\nu} \frac{(\rho_m - \rho_w)}{\rho_m} \times \\ &\left[\frac{\partial}{\partial x} \left(h^3 \frac{\partial h}{\partial x} - h^3 \sin\theta \right) + \frac{\partial}{\partial y} \left(h^3 \frac{\partial h}{\partial y} \right) \right] \end{aligned} \quad (4)$$

Assuming that the volume of the gravity current increases with time as qt^α , where α is a non-negative constant and q is the volume flux of the intruding flow (i.e. effusion rate), the mass conservation of the fluid gives:

$$\int_{x,y} \int h(x, y, t) dx dy = qt^\alpha \quad (5)$$

Note that $\alpha = 0$ corresponds to the release of a constant volume of fluid, and $\alpha = 1$ to a constant flux. In general, Eq. 4 must be solved numerically using techniques such as finite different method. Using Eq. 4, we can calculate the shape and rate of propagation of the intruding flow over an inclined surface. The special case with $\theta = 0$ (horizontal surface, Fig. 5a) is solved by Huppert (1982). His results provide a calibration for our numerical code.

Two time scales arise naturally in this system. The first is the time required to build the edifice, t_c . The other is a characteristic time scale for the flow to spread, t_s . If we consider L and H as the horizontal and vertical length scales of the flow, respectively, we obtain:

$$t_c = L^2 H / q \quad (6)$$

$$t_s = \frac{\rho_m \nu L^2}{g(\rho_m - \rho_w) H^3} \quad (7)$$

It is difficult to estimate precisely how long a submarine eruption lasts without knowing the effusion rate, and this adds to the difficulties of understanding the formation of large submarine terraces. However, subaerial ERZ eruptions have been extensively studied, and their effusion rates, $q \approx 0.1 \text{ km}^3/\text{yr}$ (Tilling and Dvorak, 1993) can be used as a starting point for our modeling. For a

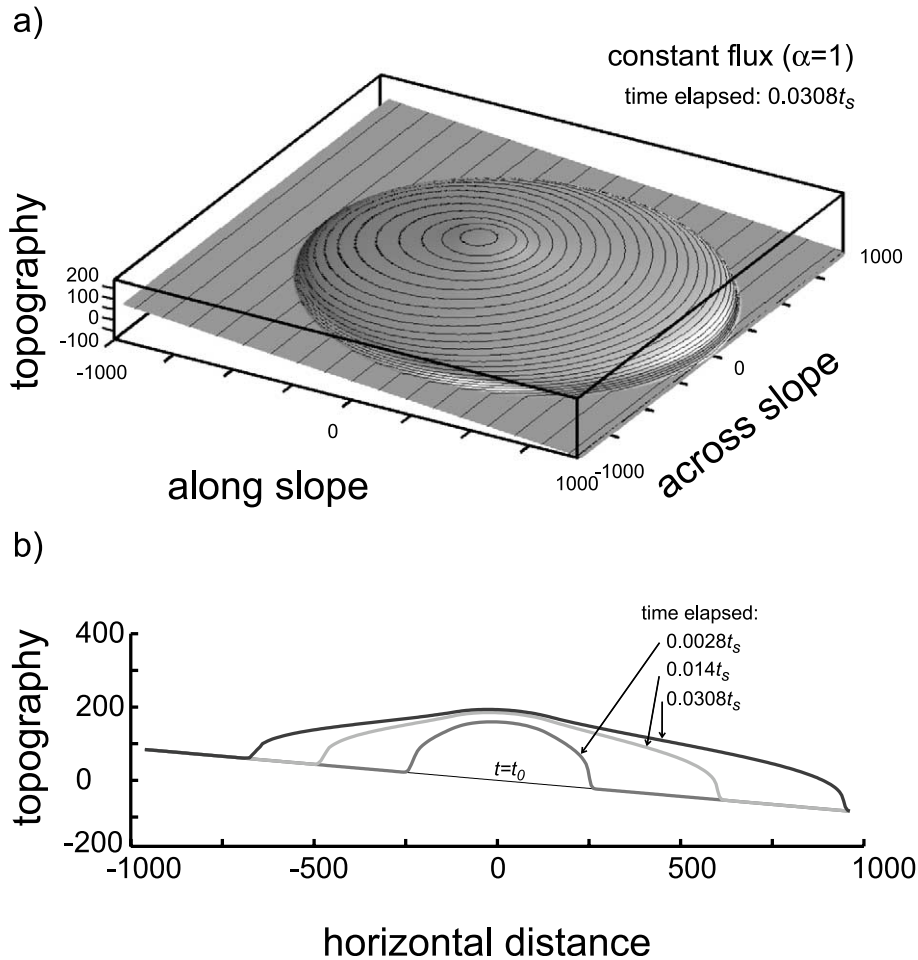


Fig. 6. (a) Simulation results of an isoviscous flow spreading on an inclined surface with a 5° slope using the constant flux model ($\alpha=1$). The contours represent the height of the lava terrace. The source function is a cylinder with finite-sized circular cross-section. Note the shape of the flow around the source (flow spreads further downhill, causing asymmetric spreading along the slope). (b) Progressive flow spreading as a function of time. In this model, the lava accumulation and spreading start simultaneously at $t=t_0$. Total lava volume accumulation can be used to calculate the time elapsed after spreading (accumulation) begins.

flow of volume $\sim 1 \text{ km}^3$, this implies $t_c \approx 10 \text{ yr}$. The spreading time, t_s , is harder to constrain a priori, because the viscosity is a strong function of temperature, and we do not model temperature effects. However, the relative importance of spreading and construction can be assessed through the scaled effusion rate

$$Q = \frac{t_s}{t_c} = \frac{q}{\frac{g(\rho_m - \rho_w)}{v} H^4} \quad (8)$$

If $Q \gg 1$, the time required for spreading is large and thus the spreading effect is insignificant compared with the accumulation rate, and lava will pile up. If $Q \ll 1$, the spreading will be very fast and it is unlikely that a terrace will be built. It is also possible to define from Eq. 8 a critical viscosity, v_c , for which $t_s \approx t_c$, or $Q \approx 1$ (i.e. the spreading and accumulation rates are comparable, and therefore lava terraces will be built). Our model indicates that the critical viscosity is a strong function of the flow thickness, H , but not

of flow length, L . For the largest terraces, $H \approx 100$ m, using $\rho_m \sim 3000 \text{ kg/m}^3$, $\rho_w = 1000 \text{ kg/m}^3$, and $q \approx 0.1 \text{ km}^3/\text{yr}$, we obtain $v_c \approx 10^8 \text{ m}^2/\text{s}$. This means that an increase of 8–10 orders of magnitude in viscosity is required to yield a terrace, as the lavas at the Puna Ridge have a tholeiitic composition (Johnson et al., 2002). This is clearly too large, which means that we cannot have a realistic model by simply incorporating variable viscosity in our theoretical predictions.

4. Simulation results

Using a source function of a cylinder with finite-sized circular cross-section, we calculated how the shape of a lava body evolves with time once it is emplaced on an inclined surface. Because the focus of this study is to quantify how effusion rate, pre-existing topographic slope, and lava volume etc. affect meso-scale lava morphology, we will present

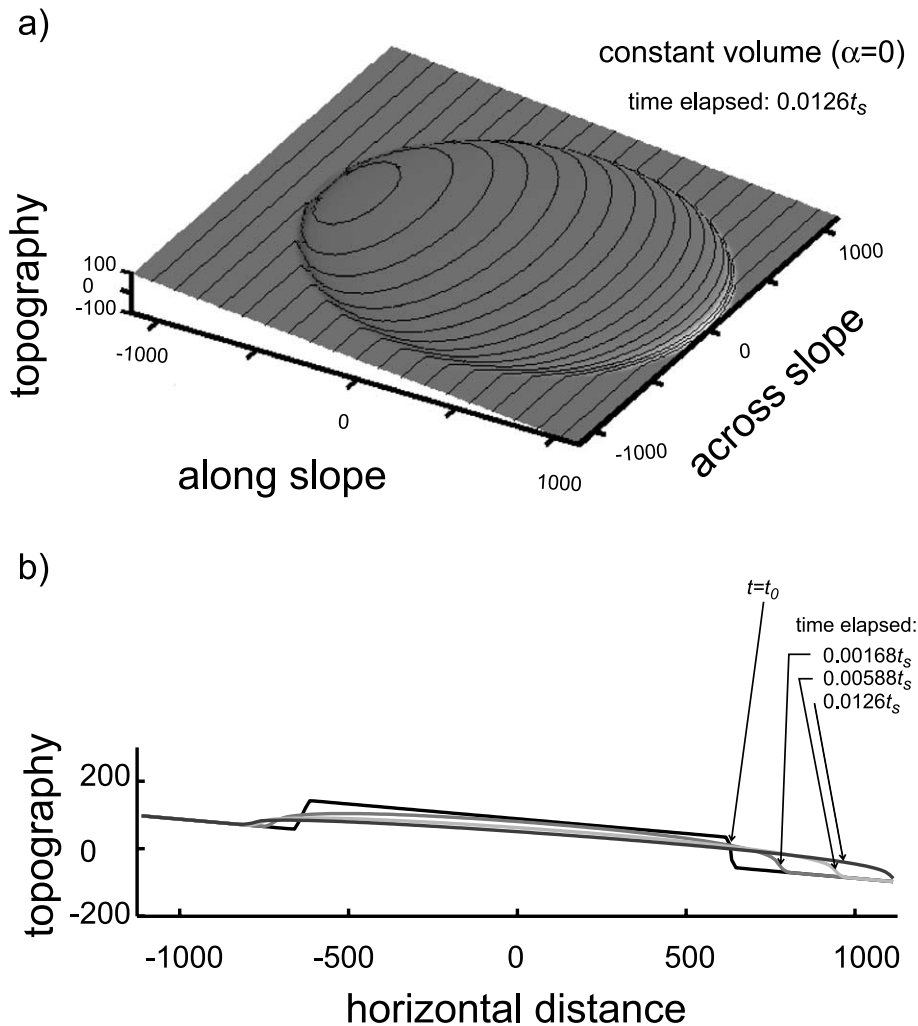


Fig. 7. (a) Simulation results of an isoviscous flow spreading on an inclined surface with a 5° slope using the constant volume model ($\alpha=0$). The contours represent the height of the lava terrace. Note that the thickness of the flow is smaller and the flow shape is more asymmetric along the slope, compared to the results from a constant flux model shown in Fig. 6. (b) Progressive flow spreading as a function of time. In this model, the spreading of the lava starts after lava accumulation is completed ($t = t_0$). Total lava volume remains the same during spreading. The time elapsed after spreading begins can be scaled to the initial time.

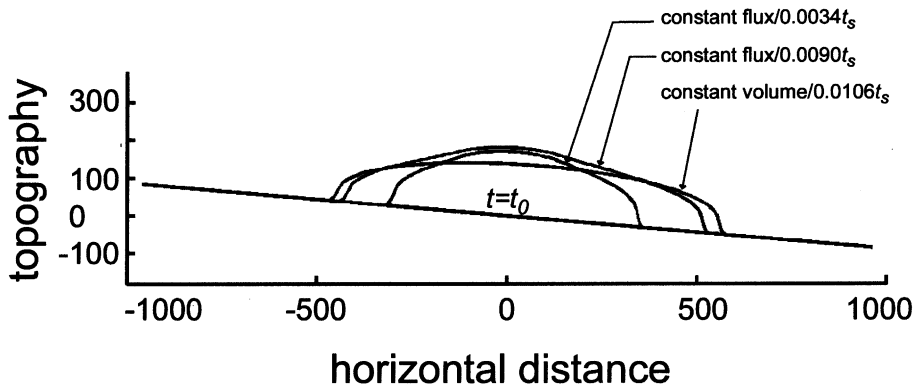


Fig. 8. Simulation results of an isoviscous flow spreading on an inclined surface with a 5° slope using the hybrid model. In this model, we start with the constant flux model (accumulation plus relaxation) that results in the flow profiles marked as constant flux/ $0.0034t_s$ and $0.0090t_s$. We then switch to the constant volume model (relaxation only), using the constant flux/ $0.0090t_s$ as input. The flow shape produced by the hybrid model shows a better agreement with the shape of submarine terraces in Fig. 2c.

our modeling results in dimensionless quantities.

If we assume that the eruption pattern can be approximated by a constant flux model ($\alpha=1$), the accumulation of the lava volume happens simultaneously while it is spreading along the slope. The shape of the submarine flow after emplacement over an inclined plane with a slope of 5° is shown in Fig. 6. Alternatively, we can choose to simulate the emplacement of lava terraces with the constant volume model ($\alpha=0$), using again a cylinder centered at $(x=0, y=0)$ as the initial shape of the lava body and model the subsequent spreading of the edifice. The initial shape does not have visible effects on the final product because the gravitational spreading quickly removes any preexisting shape.

Comparison of Figs. 6 and 7 shows that eruption style plays an important role in determining the shape of the lava body. If the effusion rate is high and the duration of eruption is short (constant volume model, $\alpha=0$), the lava will be both thinner and more asymmetric along the slope. If the effusion rate is low and the duration of eruption is long (constant flux model, $\alpha=1$), the lava is more likely to form a thicker and more symmetric shape (i.e. terraces). In reality, the eruption history may be better described as the combination of the above two end-member cases. Combining constant flux and constant flow models, we

also construct a hybrid model. We take the results of the constant flux model ($\alpha=1$) in Fig. 6, and then let the lava body spread using the constant volume model ($\alpha=0$). Using this hybrid model the average α is between 0 and 1. The shape of the lava body generated using the hybrid model is shown in Fig. 8. The results of the hybrid model are the closest match to the shape of submarine terraces.

The effect of regional slope on the spreading of viscous flow is shown in Fig. 9. In Fig. 10, the up- and downslope distances that lava spreads at submarine conditions are compared to the lava spreading at subaerial conditions (i.e. density and viscosity of water vs. those of air).

Though none of the models produces a horizontal top, this study has helped us in quantifying: (1) how the interplay of the competing processes of flow construction and spreading affects the flow shape; (2) how the flow shape also depends on the regional slope θ ; and (3) how the flow relaxation is facilitated by low viscosity, high effusion rate and high fluid density contrast. The simulation results indicate that, in general, the constant flux model (Fig. 6) gives better results in simulating the semi-circular terraces than the constant volume model (Fig. 7) does. The steeper the slope ($\theta \geq 10^\circ$), the less likely it is that semi-circular features will form (Fig. 10). It is also true that the density, viscosity, and the submarine

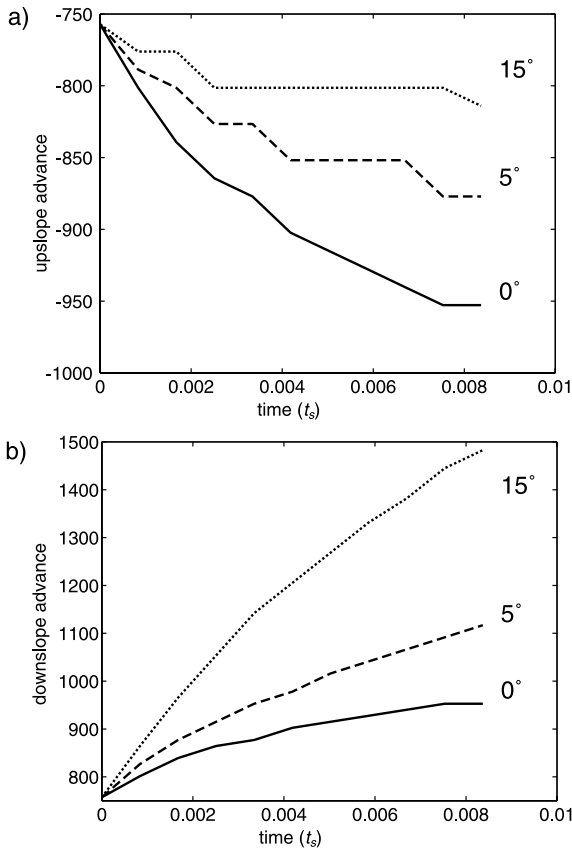


Fig. 9. Position of (a) downslope and (b) upslope limits of a constant volume flow spreading on a horizontal surface (solid line) or with underlying slope of 5° (dashed line) or 15° (dotted line). With steeper slopes, upslope advance is suppressed, and the flow becomes more elongated and asymmetric in plan shape.

pressure and temperature conditions make spreading of the lava at the seafloor slower than that in air. Therefore, lava terraces are more likely to form in submarine conditions.

5. Other geological models

Several models have been previously proposed to explain the flat-topped shape of volcanoes. For example, eruptions could be confined to circumferential vents and spill inward and build up to form a flat-topped feature. Alternatively, the flat top may form during a sequence of events that

starts with the development of summit craters and calderas, followed by the building of summit plateaus, and then the infilling of the summit depressions (Simkin, 1972). As a test for the first case, we find no evidence for circumferential vents feeding the submarine terraces that we have seen. In contrast to the second hypothesis, most of the summit depressions that we have observed are much smaller than the flat tops. As mentioned, summit craters most likely represent drainback features of portions of the still molten interior of the volcanoes. Several episodes of drainback and infilling could occur. Nonetheless, for simplicity, our initial modeling attempts assume that drainback and collapse do not fundamentally affect the final shape of the terraces.

Three other models may be more relevant for the formation of submarine terraces. The first one is the perched lava pond model described by Wilson and Parfitt (1993) for features emplaced on the subaerial ERZ. Perched lava ponds form when a channelized flow encounters a decrease in slope. Thin lava flows move radially outwards and expand until reaching a critical radius that is

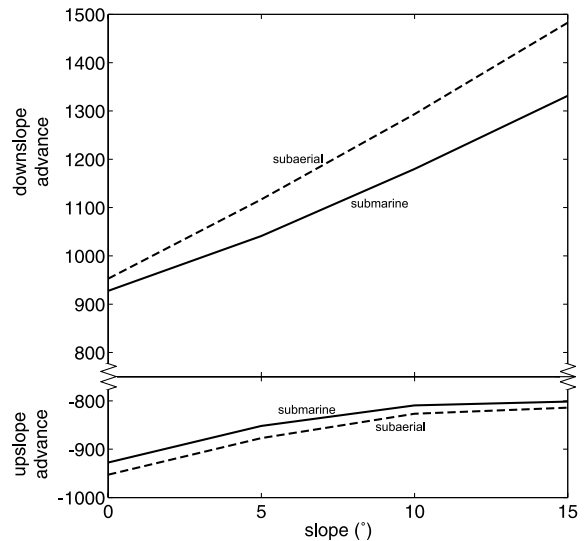


Fig. 10. Position of downslope and upslope limits of a constant volume flow spreading as a function of the underlying slope under both submarine (solid lines) and subaerial (dashed lines) conditions. The flow limits are at ± 757.2 at $t = 0$.

controlled by flow rate and cooling rate. The final shape is that of a flat-topped semi-circular volcano with steep flanks (Wilson and Parfitt, 1993). On the subaerial ERZ, perched lava ponds are typically less than a few hundred meters in diameter and a few meters high. The largest Puna Ridge terraces are one order of magnitude larger in diameter and two orders of magnitude larger in height. Thus the Wilson and Parfitt model would require effusion rates of several hundred cubic meters per second to form these larger features (Smith and Cann, 1999). Whether these effusion rates are reasonable for long periods of time in the submarine environment is not known, but they are rare subaerially.

Another model proposed by Gregg and Chadwick (1996) is based on the formation of lava pillars as lava is emplaced within the axial summit collapse trough of the East Pacific Rise. In this model, the formation of lava pillars begins with the emplacement of initially thin, slow-moving lobate lava flows. At submarine conditions the rapid initial rate of crust growth on basaltic flows means that the flow is confined by the strength of the solid crust. This impedes the lateral advance of the flow. Continuing lava injection into the flow interior causes the uplift of the top crust, and the flow thickens. Although their model describes much smaller features than the terraces, inflation may be important in forming submarine terraces as well.

The third and most recent model that is directly applicable to the formation of submarine terraces was proposed by Clague et al. (2000). Based on detailed observations of these features on the submerged upper flanks and rift zones of Hawaiian volcanoes, Clague et al. (2000) suggested that terraces form as a consequence of a continuously overflowing submarine lava lake that builds consecutive levees that buttress the lava. They concluded that these flat-topped submarine features formed during long-lived, steady, effusive, point source eruptions on gentle slopes.

Our numerical model provides a useful tool to quantify the input parameters to test the geological models presented above. Based on the inflation mechanism similar to that proposed by Gregg and Chadwick (1996), our modeling results

demonstrate quantitatively why low effusion rate, gentle regional slope, and submarine conditions favor the formation of large lava terraces. The consistency between our modeling results and the eruption conditions specified by Clague et al. (2000) demonstrates that the simple isoviscous model used in this study captured some of the most important physics that controls the formation of the submarine terraces.

6. Discussion

In this study, we use the Newtonian flow rheology to study the emplacement of submarine lava terraces. While the Newtonian model is oversimplified and cannot characterize many complex geological details, it is a good first-order approximation for studying tholeiitic lavas, if the cooling is slow enough (due to a large heat budget, or a small temperature difference, or low cooling efficiency), or cooling effects are confined in a small part of a lava body (Gregg and Greeley, 1993; Gregg and Fornari, 1998). Clague et al. (1995) report that the Puna Ridge is covered with tholeiitic lavas with viscosities ranging from 20 to 170 Pa s. Recent electron microprobe major and minor element data for volcanic glass samples collected during our cruise show similar tholeiitic lava compositions (Johnson et al., 2002). Given these viscosities and compositions, Newtonian flow rheology is a good approximation for the lava.

At submarine temperatures, a thin brittle shell may form at the outer layer of a lava body as it is emplaced (Gregg and Greeley, 1993; Gregg and Fornari, 1998). If, compared with the thickness of the lava body, the brittle shell is thin and has very little strength, it is then reasonable to assume that the formation of lava terraces is largely controlled by the low viscosity lava body beneath the shell. A brittle shell may also slow down further heat loss deep inside the lava body (e.g. Gregg and Greeley, 1993), so that the isoviscous model used in this study is a reasonable approximation.

Assuming the terraces are made of basaltic lava (Clague et al., 1995; Johnson et al., 2002), a spreading time, t_s , can be estimated. For the largest terrace ($H = 100$ m, $L = 1$ km), the viscosity of

tholeiitic lava ($\sim 0.033 \text{ m}^2/\text{s}$ at liquidus temperature) leads to the spreading time of $t_s \approx 5 \times 10^{-5}$ s. Such a minuscule time scale means the spreading will be very fast and no high-relief features should be expected on the Puna Ridge. Therefore, the presence of large terraces implies that the average lava viscosity of the whole flow is several orders of magnitude higher than $\sim 0.033 \text{ m}^2/\text{s}$, and thus, that cooling plays a critical role in forming those lava terraces. As cooling proceeds, the flow viscosity, and with it the spreading time scale (t_s , Eq. 7) increases. The fact that these features are restricted to the submarine portion of the ERZ may indicate that enhanced cooling in the submarine environment is required for building terraces. Incorporating cooling effects (increased lava viscosity) into the model will also help to address other problems. A major shortcoming of the current isoviscous flow model is that it does not include a stopping mechanism. Given enough time, the flow will eventually become a thin flat layer along the spreading surface. Cooling effects will provide a straightforward way to remedy this situation.

Cooling due to heat diffusion has been included in other gravity-driven lava flow models (Bercovici, 1994; Bercovici and Lin, 1996; Sakimoto and Zuber, 1995; Bruno et al., 1996) and could be included in ours as well. However, diffusive cooling may not be appropriate for a large lava body as temperature variations are likely confined to near the surface of the lava body. If large heat loss occurs near the surface of the whole lava body, it is easy to envision that a region with high crystallinity may develop near the flow surface. Thus, Bingham yield strength will affect the flow formation (Lionel Wilson, personal communication).

Many observations of lava flows indicate that during the active stage of eruption a thin crust will form at the surface of the flow due to cooling as we mentioned above (Gregg and Greeley, 1993; Gregg and Fornari, 1998). Although the crust may be thin and have relatively low strength at the beginning, the effect of a crust may not be negligible over a long period of time. Iverson (1990) proposed a conceptual model that treats lava domes as brittle shells that enclose pressur-

ized lava. His model provides a new dimension to the modeling of lava domes by imposing an explicit mechanism of tensile failure for eruptive dome growth. To account for effects of non-Newtonian rheology and brittle shells on lava flows and domes, our future plans are to develop more sophisticated models following the ideas of Liu and Mei (1989), Blake (1990), Iverson (1990), Griffiths and Fink (1993, 1997) and Fink and Griffiths (1998).

Laboratory simulations provide accurate analogs of submarine lava terrace emplacement and have increased our understanding of these processes. To test and refine the numerical models described above, laboratory simulations using experimental methods employed by Fink and Griffiths (Fink and Griffiths, 1990; Griffiths and Fink, 1992; Gregg and Fink, 1995, 2000) should be conducted.

Acknowledgements

Discussions with Joe Cann, Lionel Wilson, Tracy Gregg, and Elisabeth Parfitt helped clarify various aspects of the manuscript. Comments and suggestions from Susan Sakimoto, Lionel Wilson, and an anonymous reviewer helped to improve the manuscript. W.Z. thanks the support from the J. Lamar Worzel Assistant Scientist Fund and The Penzance Endowed Fund in Support of Assistant Scientists at WHOI. This research was partially supported by the National Science Foundation under Grants OCE-9618226 and OCE-9986456.

References

- Bercovici, D., 1994. A theoretical model of cooling viscous gravity currents with temperature-dependent viscosity. *Geophys. Res. Lett.* 21, 1177–1180.
- Bercovici, D., Lin, J., 1996. A gravity current model of cooling mantle plume heads with temperature-dependent buoyancy and viscosity. *J. Geophys. Res.* 101, 3291–3309.
- Blake, S., 1990. Viscoplastic models of lava domes. In: Fink, J.H. (Ed.), *Lava Flows and Domes: Emplacement Mechanisms and Hazard Implication*. Springer Verlag, Berlin, pp. 88–126.
- Bruno, B.C., Baloga, S.M., Taylor, G.J., 1996. Modeling grav-

- ity-driven flows on an inclined plane. *J. Geophys. Res.* 101, 11565–11577.
- Chadwick, W.W., Jr., Embley, R.W., 1998. Graben formation associated with recent dike intrusions and volcanic eruptions on the mid-ocean ridge. *J. Geophys. Res.* 103, 9807–9825.
- Clague, D.A., Moore, J.G., Dixon, J.E., Friesen, W.B., 1995. Petrology of submarine lavas from Kilauea's Puna Ridge, Hawaii. *J. Petrol.* 36, 299–349.
- Clague, D.A., Moore, J.G., Reynolds, J.R., 2000. Formation of submarine truncated volcanic cones in Hawaii. *Bull. Volcanol.* 62, 214–233.
- Fink, J.H., Griffiths, R.W., 1990. Radial spreading of viscous-gravity currents with solidifying crust. *J. Fluid Mech.* 221, 485–509.
- Fink, J.H., Griffiths, R.W., 1998. Morphology, eruption rates, and rheology of lava domes: insight from laboratory models. *J. Geophys. Res.* 103, 527–545.
- Gregg, T.K.P., Chadwick, W.W., Jr., 1996. Submarine lava-flow inflation: A model for the formation of lava pillars. *Geology* 24, 981–984.
- Gregg, T.K.P., Fink, J.H., 1995. Quantification of submarine lava-flow morphology through analog experiments. *Geology* 23, 73–76.
- Gregg, T.K.P., Fink, J.H., 2000. A laboratory investigation into the effects of slope on lava flow morphology. *J. Volcanol. Geotherm. Res.* 96, 145–159.
- Gregg, T.K.P., Fornari, D.J., 1998. Long submarine lava flows: Observations and results from numerical modeling. *J. Geophys. Res.* 103, 27517–27531.
- Gregg, T.K.P., Greeley, R., 1993. Formation of Venus canali: Consideration of lava types and their thermal behaviors. *J. Geophys. Res.* 98, 10873–10882.
- Griffiths, R.W., Fink, J.H., 1992. Solidification and morphology of submarine lavas: a dependence on extrusion rate. *J. Geophys. Res.* 97, 19729–19737.
- Griffiths, R.W., Fink, J.H., 1993. Effects of surface cooling on the spreading of lava flows and domes. *J. Fluid Mech.* 252, 667–702.
- Griffiths, R.W., Fink, J.H., 1997. Solidifying Bingham extrusions: A model for the growth of silicic lava domes. *J. Fluid Mech.* 347, 13–36.
- Haymon, R.M., Fornari, D.J., Von Damm, K.L., Lilley, M.D., Perfit, M.R., Edmond, J.M., Shanks, W.C., III, Lutz, R.A., Grebmeier, J.M., Carbotte, S., Wright, D., McLaughlin, E., Smith, M., Beedle, N., Olson, E., 1993. Volcanic eruption of the mid-ocean ridge along the East Pacific Rise crest at 9°45'–52'N: Direct submersible observations of seafloor phenomena associated with an eruption event in April 1991. *Earth Planet. Sci. Lett.* 119, 85–101.
- Huppert, H.E., 1982. The propagation of two-dimensional and axisymmetric viscous gravity currents over a rigid horizontal surface. *J. Fluid Mech.* 121, 43–58.
- Huppert, H.E., Shepard, J.B., Sigurdsson, H., Sparks, R.S.J., 1982. On lava dome growth with application to the 1979 lava extrusion on the Soufriere of St Vincent. *J. Volcanol. Geotherm. Res.* 14, 199–222.
- Iverson, R.M., 1990. Lava domes modeled as brittle shells that enclose pressurized magma, with application to Mount St. Helens. In: Fink, J.H. (Ed.), *Lava Flows and Domes: Emplacement Mechanisms and Hazard Implications*. Springer Verlag, Berlin, pp. 47–69.
- Johnson, K., Reynolds, J., Smith, D., Kong, L., Vonderhaar, D., 2002. Petrological systematics of submarine lavas from the Puna Ridge, Hawaii: Implications for rift zone plumbing and magmatic processes. In: Takahashi, E. et al. (Eds.), *Evolution of Hawaiian Volcanoes: Recent Progress in Deep Underwater Research*. AGU Monograph, Washington, DC, pp. 143–160.
- Lister, J.R., 1992. Viscous flows down an inclined plane from point and line sources. *J. Fluid Mech.* 242, 631–653.
- Liu, K.F., Mei, C.C., 1989. Slow spreading of a sheet of Bingham fluid on an inclined plane. *J. Fluid Mech.* 207, 505–529.
- Monterey Bay Aquarium Research Institute Mapping Team, 2000. MBARI Hawaii Multibeam Survey, version 1, Monterey Bay Aquarium Research Institute, CA.
- Moore, J.G., Chadwick, W.W., Jr., 1995. Offshore geology of Mauna Loa and adjacent areas, Hawaii. In: Rhodes, J.M., Lockwood, J.P. (Eds.), *Mauna Loa Revealed: Structure, Composition, History, and Hazards*. AGU Monograph, Washington, DC, pp. 21–44.
- Moore, J.G., Phillips, R.L., Grigg, R.W., Peterson, D.W., Swanson, D.A., 1973. Flow of lava into the sea, 1969–1971, Kilauea Volcano, Hawaii. *Geol. Soc. Am. Bull.* 84, 537–546.
- Pavri, B., Head, J.W., Klose, K.B., III, Wilson, L., 1992. Steep-sided domes on Venus: Characteristics, geologic setting, and eruption conditions from Magellan data. *J. Geophys. Res.* 97, 13445–13478.
- Perfit, M.R., Chadwick, W.W., Jr., 1998. Magmatism at mid-ocean ridges: Constraints from volcanological and geochemical investigations. In: Buck, W.R., Delaney, P.T., Karson, J.A., Lagabrielle, Y. (Eds.), *Faulting and Magmatism at Mid-Ocean Ridges*. AGU Monograph, Washington, DC, pp. 59–116.
- Sakimoto, S.E.H., Zuber, M.T., 1995. The spreading of variable viscosity axisymmetric radial gravity currents: Applications to the emplacement of Venus 'Pancake' domes. *J. Fluid Mech.* 301, 65–77.
- Simkin, T., 1972. Origin of some flat-topped volcanoes and guyots. *Geol. Soc. Am. Mem.* 132, 183–193.
- Smith, D.K., Cann, J.R., 1999. Constructing the upper crust of the Mid-Atlantic Ridge: A reinterpretation based on the Puna Ridge, Kilauea Volcano. *J. Geophys. Res.* 104, 25379–25399.
- Smith, D.K., Kong, L.S., Johnson, K.T.M., Reynolds, J., and the cruise participants of TN084, 2002. Volcanic structure of the Puna Ridge, Kilauea Volcano. In: Takahashi, E. et al. (Eds.), *Evolution of Hawaiian Volcanoes: Recent Progress in Deep Underwater Research*. AGU Monograph, Washington, DC, pp. 125–142.
- Tilling, R.I., Christiansen, R.L., Duffield, W.A., Endo, E.T., Holcomb, R.T., Koyanagi, R.Y., Peterson, D.W., Unger, J.D., 1987. The 1972–1974 Mauna Ulu eruption, Kilauea

- Volcano; an example of quasi-steady-state magma transfer. In: Decker, R.W., Wright, T.L., Stauffer, P.H. (Eds.), *Volcanism in Hawaii*, pp. 405–469.
- Tilling, R.I., Dvorak, J.J., 1993. Anatomy of a basaltic volcano. *Nature* 363, 125–133.
- Walker, G.P.L., 1991. Structure, and origin by injection under surface crust, of tumuli, ‘lava rises’, ‘lava-rise pits’, and ‘lava-inflation clefts’ in Hawaii. *Bull. Volcanol.* 53, 546–558.
- Wilson, L., Parfitt, E.A., 1993. The formation of perched lava ponds on basaltic volcanoes: the influence of flow geometry on cooling-limited lava flow lengths. *J. Volcanol. Geotherm. Res.* 56, 113–123.